2D Affine Invariant Fiducial Points and Affine Absolute Invariants for Shape Matching under Affine and Weak Perspective Transformations

Fernand S. Cohen, and **C. Pintavirooj***, Member

ABSTRACT

In this paper we derive novel fiducial points on curves that are preserved under affine and weak perspective transformations, are local, intrinsic and computed from the differential geometry of the curve. These are used in a non-iterative geometric-based method for shape matching and 2D registration in the presence of affine or nonlinear transformations that can be approximated by piece wise affine transformations. To reduce the sensitivity of the computation of the fiducial points to noise, we use a B-Spline curve representation that smooths out the curve prior to the computation of these invariant points. The matching is achieved by establishing correspondences between fiducial points after a sorting based on derived set absolute local affine invariants. The performance of the matching based on these fiducial points is shown for a variety of object matching problems, and is shown to be robust and promising even in the presence of noise.

Keywords: Fiducial points; Affine absolute invariants; Affine transform; Perspective transform

1. INTRODUCTION

Shape matching is a central problem in visual information system, computer vision, pattern recognition image registration, and robotics. Application of shape matching includes image retrieval, industrial inspection, stereo vision, and fingerprint matching. The term shape is referred to the invariant geometrical properties of the relative distance among a set of static spatial features of an object. These static spatial features are known as shape features of the object. After extracting the shape features for a model and a scene, a similarity may be used to compare the shape features. The similarity measure is referred to as a shape measure. The shape measure should be invariant under certain class of geometric transformation of the object. In the simple scenario, shape measures are invariant to translation rotation and scale. In this case, the shape measures are invariant under similarity transformation. When included the invariance of shape measures to shear effect, the shape measures are said to be invariant under affine transformation. Finally in the complicated case, shape measures are invariant under perspective transformation when included the effect caused by perspective projection.

There are many techniques available to shape matching which can be classified mainly into two main categories; a global method and a local method. The global method works on an object as a whole; while the local method on a partially visible object or occlusion. Wavelet transform [1][2] is the well-known global method that transforms the image from color information in spatial domain to color variation information in frequency domain. A set of wavelet coefficients can be used as shape features for shape matching. As wavelet-transform method is based on global image transform, it is hence not robust against occlusion. Moment-based approach is other global methods that work on the whole area of an object. Based on the moment, a number of functions, moment invariant, can be defined that are invariant under similarity transformation [3][4] and affine transformation [5]. Moment-based approach also suffers from problem of noise and occlusion. Rather than working on the area of the object, the boundary can be used instead as a mean to present the pertinent information about an object is contained in the shape of its boundary. Fourier descriptors [6][7][8] and Median Axis Transformation [9][10][11] are well-known boundary representations that provide global similarity measures applied to shape matching.

Global method provides global features that are relatively stable to external noise, however, they are not robust to occlusion and, more importantly, global features of two similar shapes differ slightly. On the contrary, while local features are insensitive to occlusion, they are sensitive to noise and the amount of local information available is usually insufficient for robust matching. Most of the local features exploit geometric properties of contour that remain unchanged under certain class of geometric transformation - the so-called geometric invariant [12][13][14]. Curvature is local geometric invariant that has been used extensively in shape matching for its ability to carry information at varying resolution. Although curvature is invariant under similarity transformation, it

Manuscript received on July 1, 2009.
* Corresponding author.
Fernand S. Cohen is with Department of Electrical and Computer Engineering Drexel University Philadelphia, PA 19104
C. Pintavirooj is with Faculty of Engineering, King Mongkut's Institute of Technology Ladkrabang Bangkok 10520, Thailand. *E-mail addresses:* kpchucha@kmitl.ac.th

is not preserved under affine transformation. To bypass this problem, many literatures concentrated on using only curvature extremal point [15]-[20] that is insensitive to affine transformation. The curvature extremal points include the high-curvature points or the corner points and zero-curvature point or inflection points. The high-curvature points are not affine invariant; yet they are robust to affine transformation and have been used extensively for shape matching. The zero-curvature points have been proved that they are affine invariant [21] and applied for numerous applications not only in shape matching but in various contexts as well. The zero-curvature points have a major drawback in that they are sensitive to noise. To provide the similarity measures, the curvature extremal point usually must combine with other geometric invariant such as the area bounded by three selective curvature extremal points [21][22]. The area is a well-known relatively affine invariant. To obtain an absolute invariant, a ratio of two areas is computed and used as a good candidate for similarity measures. Other typical geometric features include line intersections [23], and [24], centroids of closed-boundary region [25], knot points [26], etc.

There are different approaches for curve modeling such as Fourier descriptor [27][28], chain code [29], polygon approximation [20], curvature primal sketch [31], medial axis transformation [32], autoregressive model [33][34], moment [35][36][37], parametric algebraic curve [38], curvature invariant [39], stochastic transformation [40], implicit polynomial function [41], bounded polynomial [42], B-Spline [43][44], and reaction diffusion [45]. Among others, B-Spline stands as of one the most efficient curve representation and processes very attractive properties such as spatial uniqueness, boundedness and continuity, local shape controllability and invariance to affine transformation.

In this paper we introduce a novel shape measure which is not only preserved under affine transformation but also robust under weak perspective transformation. There are three main contributions to this paper. Firstly, we introduce a novel set of local intrinsic fiducial points which are derived from the derivative of the object curve and their derivatives and are preserved under affine and weak perspective. Secondly, we construct absolute invariants for planar curves that are preserved under affine transformations and an invariant for perspective transformations. Our similarity measure is based on using a five selective fiducial points to compute the well-known five-point coplanar invariant. Five-point coplanar invariant is based on using ratio of ratio of volume. It is hence an absolute perspective invariant and hence very suitable to be used to match planar curves. Finally, to bypass the problem of noise for both the data presentation as well as the computation of these invariants, we model the external contour of the object with the approximating B-Spline curve representation that are themselves preserved under affine and weak perspective transformations and are robust to noise both local and global [21][50]. Hence the selection of the B-Spline curve allows for the reduction of the sensitivity of the fiducial points to noise as well as it provides an analytic solution to curvature computation.

This paper is organized as follows. Section 2 introduces the local geometric curve features used as fiducial points or fiducial points on the curve. Section 3 shows how to construct absolute invariant from set of geometric curve features. Section 4 describes how to establish the correspondence between two sets of feature points. B-Splines curves are given in section 5. Experimental results are shown in section 6. Discussion and conclusion are presented in section 7.

2. INTRINSIC GEOMETRIC FEATURES OF CURVE

Local and invariant intrinsic properties are provided by the Frenet frames [46], which states that for a curve $r(s)$ parameterized by arc length s, the tangent $t(s) = r^{(1)}(s)$, the curvature $k(s) = r^{(2)}(s)$, the vector $b(s) = t(s)xk(s)$, and the torsion $\tau(s) = - < r^{(2)}(s), b^{(1)}(s) >$ determines as set of local coordinates on the curve at each point that completely characterizes the curve at that point, where $r^{(k)}(s)$stands the k^{th} order derivative of r with respect to s, and x is the cross product operation. As we are interested in finding the relative and absolute invariant to the affine transformation, we observe that since arc length is not preserved under the affine transformation, neither $t(s)$ nor $b(s)$ cannot be used as they are not relative invariants. The parameter s can also be replaced by any other one-to-one parameterization with s. For instance, we can parameterize the curve by the parameter t, which could be the time it took a particle traveling on the curve to reach the position $r(t)$, in that case $s = \int_0^t ||r^{(1)}(t)||dt$, where $||r^{(1)}(t)||$ is the speed of the particle at time t.

2.1 Relative Affine Invariant Intrinsic Curve Points

Let $r(t) = [x(t), y(t)]$, where t is a parameter, represent a shape (or curve) C in Cartesian coordinate system. The curvature $k(t)$ of the shape C is hence define as

$$k(t) = \frac{|r^{(1)}(t) \times r^{(2)}(t)|}{|r^{(1)}(t)|^3} = \frac{\dot{x}(t)\ddot{y}(t) - \ddot{x}(t)\dot{y}(t)}{(\dot{x}(t) + \dot{y}(t)^2)^{3/2}} \quad (1)$$

$$where\ \dot{x}(t) = \frac{dx(t)}{dt}, \ddot{x}(t) = \frac{d^2x(t)}{dt^2}, \dot{y}(t) = \frac{dy(t)}{dt},$$

$$and\ \ddot{y}(t) = \frac{d^2y(t)}{dt^2}$$

Let $C_a = r_a(\tau) = [u(\tau), v(\tau)]$, where τ is a parameter, be an affine-transformed version of the shape C. Mathematically, the relation between two shapes C and $C^{'}$ under affine transformation can be expressed as follow

$$\begin{bmatrix} u(\tau) \\ v(\tau) \\ 1 \end{bmatrix} = \begin{bmatrix} a_{11} & a_{12} & b_1 \\ a_{21} & a_{22} & b_2 \\ 0 & 0 & 1 \end{bmatrix} \begin{bmatrix} x(t) \\ y(t) \\ 1 \end{bmatrix} \quad (2)$$

where $a_{ij}, i = 1:2, j = 1:2$ are affine transformed parameter associated with rotation, scale and shear and $b_i, i = 1:2$ is affine transformed parameter associated with translation. The curvature of the affine-transformed shape is

$$k_a(t) = \frac{|r_a^{(1)}(t) \times r_a^{(2)}(t)|}{|r_a^{(1)}(t)|^3} = \frac{\dot{u}(t)\ddot{v}(t) - \ddot{u}(t)\dot{v}(t)}{(\dot{u}(t) + \dot{v}(t)^2)^{3/2}} \quad (3)$$

$$where\ \dot{u}(t) = \frac{du(t)}{dt}, \ddot{u}(t) = \frac{d^2u(t)}{dt^2}, \dot{v}(t) = \frac{dv(t)}{dt},$$

$$and\ \ddot{v}(t) = \frac{d^2v(t)}{dt^2}$$

The nominator term of equation (1) is equivalent to one half of the area bounded by the vectors $r^{(1)}(t)$ and $r^{(2)}(t)$; while that of equation (3) is equivalent to one half of the area bounded by vector $r_a^{(1)}(t)$ and $r_a^{(2)}(t)$. The denominator of equation (1) is the length of vector $r^{(1)}(t)$; while that of equation (3) is the length of vector $r_a^{(1)}(t)$. Under an affine transformation, it can be shown that the nominators of equation (1) and (3) which are the area are related by determinant of transformation matrix and hence relative invariant, i.e.

$$\begin{vmatrix} \dot{u}(t) & \ddot{u}(t) \\ \dot{v}(t) & \ddot{v}(t) \end{vmatrix} = \begin{vmatrix} a_{11} & a_{12} \\ a_{21} & a_{22} \end{vmatrix} \begin{vmatrix} \dot{x}(t) & \ddot{x}(t) \\ \dot{y}(t) & \ddot{y}(t) \end{vmatrix} \quad (4)$$

where $|a|$ denote determinant of a. By contrast, we can show that denominator of equation (1) and (3) is not affine invariant, i.e.

$$\left(\dot{u}(t)^2 + \dot{v}(t)^2\right)^{3/2} =$$

$$\left(\left(a_{11}\dot{x}(t) + a_{12}\dot{y}(t)\right)^2 + \left(a_{21}\dot{x}(t) + a_{22}\dot{y}(t)\right)^2 \right)^{3/2} \quad (5)$$

This expression indicated that the length of first derivative vector is not a relative invariant under the affine transformation. As a consequence, only the nominator term of the definition of curvature is the promising candidate for constructing affine invariants. In this paper we call the nominator term as the affine curvature.

Inflection points are points on the curve at which the curvature is zero, i.e., points at which

$$k(t) = \frac{|r^{(1)}(t) \times r^{(2)}(t)|}{|r^{(1)}(t)|^3} = \frac{\dot{x}(t)\ddot{y}(t) - \ddot{x}(t)\dot{y}(t)}{(\dot{x}(t) + \dot{y}(t)^2)^{3/2}} = 0$$

or the points at which

$$|r^{(1)}(t) \times r^{(2)}(t)| = \dot{x}(t)\ddot{y}(t) - \ddot{x}(t)\dot{y}(t) = 0 \quad (6)$$

As a results, $r^{(1)}(t)$ and $r^{(2)}(t)$ are parallel at the inflection point.

Inflection points on the affine transformed curve are the points at which

$$k_a(t) = \frac{|r_a^{(1)}(t) \times r_a^{(2)}(t)|}{|r_a^{(1)}(t)|^3} = \frac{\dot{u}(t)\ddot{v}(t) - \ddot{u}(t)\dot{v}(t)}{(\dot{u}(t) + \dot{v}(t)^2)^{3/2}} = 0$$

or the points at which

$$\dot{u}(t)\ddot{v}(t) - \ddot{u}(t)\dot{v}(t) = \begin{vmatrix} a_{11} & a_{12} \\ a_{21} & a_{22} \end{vmatrix} \dot{x}(t)\ddot{y}(t) - \ddot{x}(t)\dot{y}(t) = 0$$

$$\dot{x}(t)\ddot{y}(t) - \ddot{x}(t)\dot{y}(t) = 0 \quad (7)$$

which is the same as (6). As a consequence, at the inflection points, the curvature or affine curvature is zero and $r^{(1)}(t)$ and $r^{(2)}(t)$ are parallel. Since the affine map preserve parallelism, we have shown that $r_a^{(1)}(t)$ and $r_a^{(2)}(t)$ are also parallel. Therefore the inflection points of the affine transformed curve are the transformed inflection points of the original curve and hence are relative affine invariant. Inflection points were suggested by us [21] as a candidate for curve matching [21]. In this paper we augment these invariants by considering cross product terms of the curve and its various possible nonzero higher order derivatives, which are all area invariants, and hence relative affine invariants. So for instance if we take derivative of (6), we have

$$\dot{x}(t)\,\dddot{y}(t) + \ddot{x}(t)\,\ddot{y}(t) - \ddot{x}(t)\,\ddot{y}(t) - \dddot{x}(t)\,\dot{y}(t)$$

$$= \dot{x}(t)\,\dddot{y}(t) - \dddot{x}(t)\,\dot{y}(t) = |r^{(1)}(t) \times r^{(3)}(t)| = 0 \quad (8)$$

which is the point at which $r^{(1)}(t)$ and $r^{(3)}(t)$ are parallel and hence is also affine invariant. This point is the point at which the affine curvature is a maximum. We call this point the maximum affine curvature point. Compared with zero affine curvature points, the maximum affine curvature points are more robust to noise. Moreover, threshold of affine curvature can be set such that only the maximum affine curvature point of which its affine curvature exceeding the threshold is selected. As a result, maximum affine curvature points caused by local disturbance are excluded.

Table 1: *Set of Relative Affine Invariants on Curves*

Relative affine Invariant	Fiducial points related to the zero relative affine Invariant	Fiducial points related to the maximum of the Relative affine Invariant
$k_1(t)=\lvert r(t)\times r^{(1)}(t)\rvert$	$f_1(t)\equiv$ $k_1(t)=0$ $\lvert r(t)\times r^{(1)}(t)\rvert=0$	$f_2(t)\equiv$ $k_1^{(1)}(t)=0$ $\lvert r(t)\times r^{(2)}(t)\rvert=0$
$k_2(t)=\lvert r(t)\times r^{(2)}(t)\rvert$	$f_3(t)\equiv$ $k_2(t)=0$ $\lvert r(t)\times r^{(2)}(t)\rvert=0$ same as $f_2(t)$	$f_4(t)\equiv$ $k_2^{(1)}(t)=0$ $\lvert r(t)\times r^{(3)}(t)\rvert+\lvert r^{(1)}(t)\times r^{(2}(t)\rvert=0$
$k_3(t)=\lvert r^{(1)}(t)\times r^{(2)}(t)\rvert$	$f_5(t)\equiv$ $k_3(t)=0$ $\lvert r^{(1)}(t)\times r^{(2)}(t)\rvert=0$	$f_6(t)\equiv$ $k_3^{(1)}(t)=0$ $\lvert r^{(1)}(t)\times r^{(3)}(t)\rvert=0$

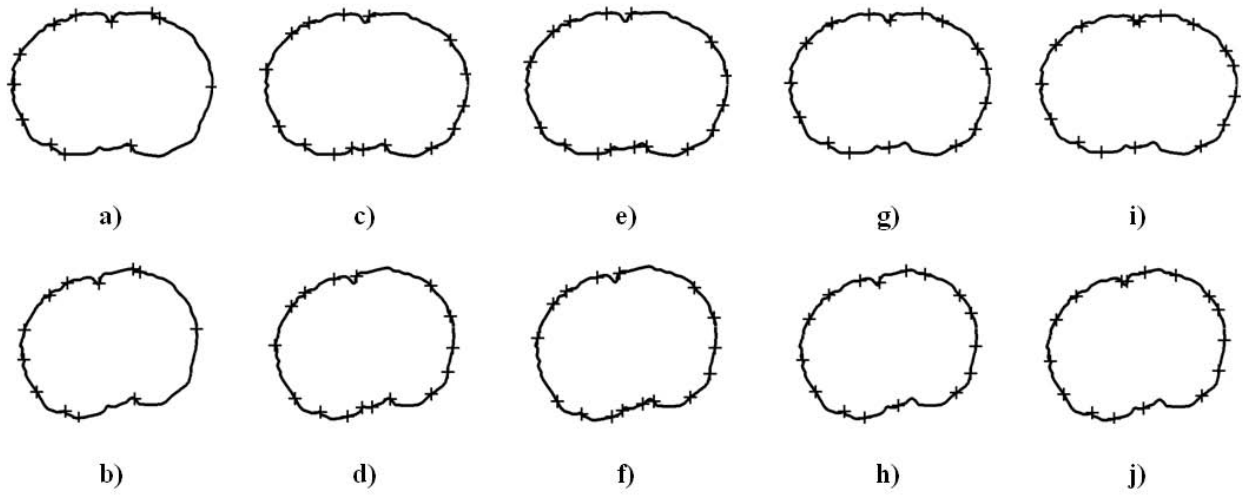

Fig.1: *show the 5 affine invariant geometric features (f_1, f_2, f_4, f_5 and f_6) residing on the original curve (a, c, e, g and i respectively) and the corresponding affine-transformed curve (b, d, f, h and j respectively)*

2.2 Augmented Set of Relative Affine Invariant Local Intrinsic Curve Points

The same concept can be applied to set of nonzero derivatives of the curve. Table 1 shows a set of geometric fiducial. When the maximum order of the derivatives of a curve used in the computation of the relative affine invariants is limited to two, in this case, we have 6 features; three of which associated with points of minimum relative affine invariant and the other three features associated with points of maximum relative affine. In the case of feature $f_4(t)$, we can proof that it is affine invariant as follows. The features on the original curve are the points where

$$k_2^{(1)}(t) = 0$$

or

$$x(t)\,\dddot{y}(t) + \dot{x}(t)\,\ddot{y}(t) - \ddot{x}(t)\,\dot{y}(t) - \dddot{x}(t)y(t) = 0$$

$$|r(t) \times r^{(3)}(t)| + |r^{(1)}(t) \times r^{(2)}(t)| = 0 \qquad (9)$$

These fiducial points on the affine transformed curve are the points at which

$$u(t)\,\dddot{v}(t) + \dot{u}(t)\,\ddot{v}(t) - \ddot{u}(t)\,\dot{v}(t) - \dddot{u}(t)v(t) =$$
$$\begin{vmatrix} a_{11} & a_{12} \\ a_{21} & a_{22} \end{vmatrix} x(t)\,\dddot{y}(t) - \dddot{x}(t)y(t) +$$

$$\begin{vmatrix} a_{11} & a_{12} \\ a_{21} & a_{22} \end{vmatrix} [\dot{x}(t)\,\ddot{y}(t) - \ddot{x}(t)y(t)] = 0$$

$$\begin{vmatrix} a_{11} & a_{12} \\ a_{21} & a_{22} \end{vmatrix} |r(t) \times r^{(3)}(t)|$$
$$+ \begin{vmatrix} a_{11} & a_{12} \\ a_{21} & a_{22} \end{vmatrix} |r^{(1)}(t) \times r^{(2)}(t)| = 0$$

$$|r(t) \times r^{(3)}(t)| + |r^{(1)}(t) \times r^{(2}(t)| = 0 \qquad (10)$$

which is the same as (9). Hence points where $k_2^{(1)}(t) = 0$ are preserved under an affine transformation. Note that the fiducial points derived from $f_1(t), f_2(t), f_3(t), f_4(t)$ (i.e., the ones that contain $r(t)$ in their computation) are only linear invariant and not affine in the case of occlusion between the object and its transformation. This is due to the fact the translation parameter b in the case would not correspond to the difference between the centroids of the curve before and after its transformation because of the occlusion. This is however, not the case for fiducial points that are derived from the curve derivatives.

3. CONSTRUCTING ABSOLUTE INVARIANT FROM FIDUCIAL POINTS ON CURVES

Geometric invariants are shape descriptors that remain unchanged under geometric transformations such as perspective and affine transformation. In this section we derive an affine absolute invariant from the fiducial points derived on curves, and show how to use these invariants to put into correspondences fiducial points before and after the transformation without ever needing to know what the values of the transformation parameters are. Once correspondences are established, the transformation parameters can then be computed using LS fitting and the objects can be aligned. These invariants can also be used as invariant object shape descriptors. We also test the five-point coplanar perspective invariant computed on the intrinsic fiducial points as a close approximation to a perspective absolute invariant, an approximation here since the fiducial points are not fully preserved under a strong perspective transformation.

3.1 Perspective Invariant

Any five nonlinear points in the plane, namely $P_1, , P_5$ can also form perspective invariant [47],[48] with their image, $P_1^{'}, ..., P_5^{'}$,

$$\frac{\left|m_{431}^{'}\right| \left|m_{521}^{'}\right|}{\left|m_{421}^{'}\right| \left|m_{531}^{'}\right|} = \frac{|m_{431}|\,|m_{521}|}{|m_{421}|\,|m_{531}|} \qquad (11)$$

where
$m_{i,j,k} = (P_i, P_j, P_k)$ with $P_i = (x_i, y_i, 1)^t$,
$m_{i,j,k}^{'} = (P_i^{'}, P_j^{'}, P_k^{'})$ with $P_i^{'} = (x_i^{'}, y_i^{'}, 1)^t$ and
$|m|$ is the determinant of m. Consider any one of the matrices in (11)

$$\begin{vmatrix} x_5 & x_1 & x_2 \\ y_5 & y_1 & y_2 \\ 1 & 1 & 1 \end{vmatrix} \quad (a)$$

$$\begin{vmatrix} x_5 & x_1 - x_5 & x_2 - x_5 \\ y_5 & y_1 - y_5 & y_2 - y_5 \\ 1 & 0 & 0 \end{vmatrix} \quad (b)$$

(12)

Equivalently, using elementary rules concerning matrices and determinant, matrix in (12.a) can be rewritten as in (12.b) which represents six times the volume of a tetrahedron shown in Figure 2 b) The formula of this volume is

$$\frac{1}{6}\,|1|\,|d_{5,1}|\,|d_{5,2}|\,sina_{12} \qquad (13)$$

where $d_{5,j}, j = 1, 2$, is the distance form the point (x_5, y_5) to the point $(x_j, y_j), |1|$ is unit length in z direction. By replacing the determinant in equation (11) with the corresponding form of equation (13), all vector magnitudes cancel, leaving only the ratio of sine of the angles, i.e.,

$$\frac{sin\ a_{12}^{'} sin\ a_{34}^{'}}{sin\ a_{14}^{'} sin\ a_{23}^{'}} = \frac{sin\ a_{12} sin\ a_{34}}{sin\ a_{14} sin\ a_{23}} \qquad (14)$$

where angle a_{ij} defined in terms of rays extended from a select point P to the remaining points $P_1, ..., P_4$ in the object plane whereas $a_{ij}^{'}$ from the selected point P' to the remaining point $P_1^{'}, ..., P_4^{'}$ in the image plane.

Since the invariant relationship in equation (14) holds under a perspective transformation, a perspective invariant can be constructed by considering 5 consecutive fiducial points which is also preserved under an affine and robust under perspective transformation. For a curve with n geometric fiducial points, there are $\binom{n}{5}$ set of absolute five-point invariants. We denoted a set of absolute five-point invariant on the original curve and affine-transformed curve as $I(k)$ and $I_a(k)$ for $k = 1, 2, .., n$ respectively.

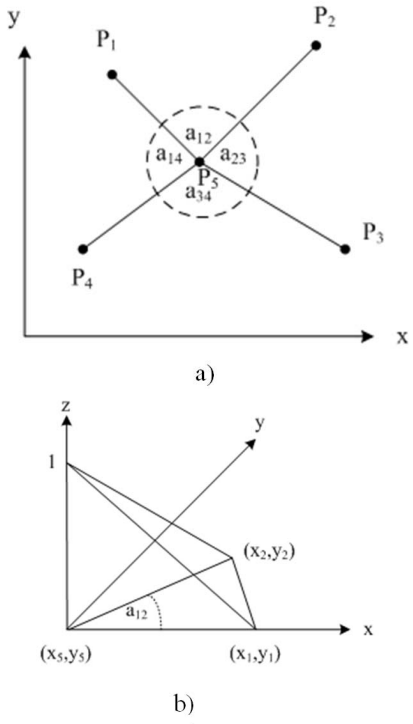

Fig.2: *a) Five coplanar points and the assigned angle. b) Determinant of matrix m_{512} is the volume of the tetrahedral bounded by $(x_5, y_5, 1), (x_1, y_1, 0)$ and $(x_2, y_2, 0)$.*

3.2 Affine Invariant

Unlike in the perspective transformation, the area is preserved under an affine transformation. A sequence of relative invariants is constructed by considering the sequences of area patch which is area of the parallelogram spanned by a set of three consecutive feature points. Denote the area patch sequence of the affine-transformed curve as $[A_a(1), .., A_a(n)]$. Area patch of the transformed curve is related to that of the original curve by the following relative invariant

$$A_a(k) = \left| \begin{array}{cc} a_{11} & a_{12} \\ a_{21} & a_{22} \end{array} \right| A(k), k = 1, 2, ..., n \qquad (15)$$

where $|A|$ is the determinant of transformation matrix. By taking the ratio of the consecutive elements of the sequence, absolute invariant is derived. Let

$$I_a(k) = \frac{\pm A_a(k)}{|A_a(k+1) \text{mod n}|} \qquad (16)$$

and

$$I(k) = \frac{\pm A(k)}{|A(k+1) \text{mod n}|} \qquad (17)$$

for $k = 1, 2, .., n$. The absolute invariant of the original curve equals to that of the transformed curve, i.e. $I_a(k) = I(k)$.

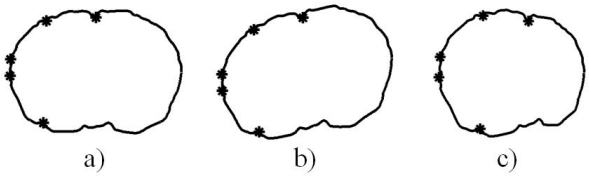

Fig.3: *a) Original sample including its maximum affine-curvature points ('*'); b) Affine transformed curved including its maximum affine -curvature points ('*'). The average area invariant error is 0.0025 and the average five-point invariant error is 0.0039; c) Perspective transformed curve including its maximum affine -curvature points ('*'). The average area invariant error is 0.1955 and the average five-point invariant error is 0.0075.*

4. ESTABLISHING CORRESPONDENCE AND ALIGNMENT

Our shape matching is based on contour registration. The registration process is carried out in the presence of an affine transformation and a possible perspective transformation. We first compute the curve intrinsic feature points. The relative invariant and absolute invariants explained in section 3 is computed. The correspondence between the feature points on the original and the transformed curve is established. From this correspondence, the transformation parameters are computed and the transformed curve is aligned against an original.

In the absence of noise, occlusion, each of $I_a(k)$ will have a counter part $I(k)$ with $I_a(k) = I(k)$, with that counterpart easily determined through a circular shift involving n comparison where n is the number of invariant. In the presence of noise and some nonlinear transformation, we allow smaller error percentage between counterpart invariant. Having a smaller threshold will force this run length matching technique to allow for only small difference between the volume patch before declares them as matching. This may reduce the length of the matched sequence element, Thus the lower the error percentage, the more strict the matching. Experimentally, an error percentage of 5% was applied. We adopted a run length method to decide on the correspondence between the two ordered set of zero-torsion points. For every starting point on the transformed, this run length method computes a sequence of consecutive invariant that satisfies $|I(k) - I_a(k)| < 0.05|I(k)|$ and declare a match based on the longest string. Once this correspondence is found, these matched fiducial points are used to estimate the polynomial transformation.

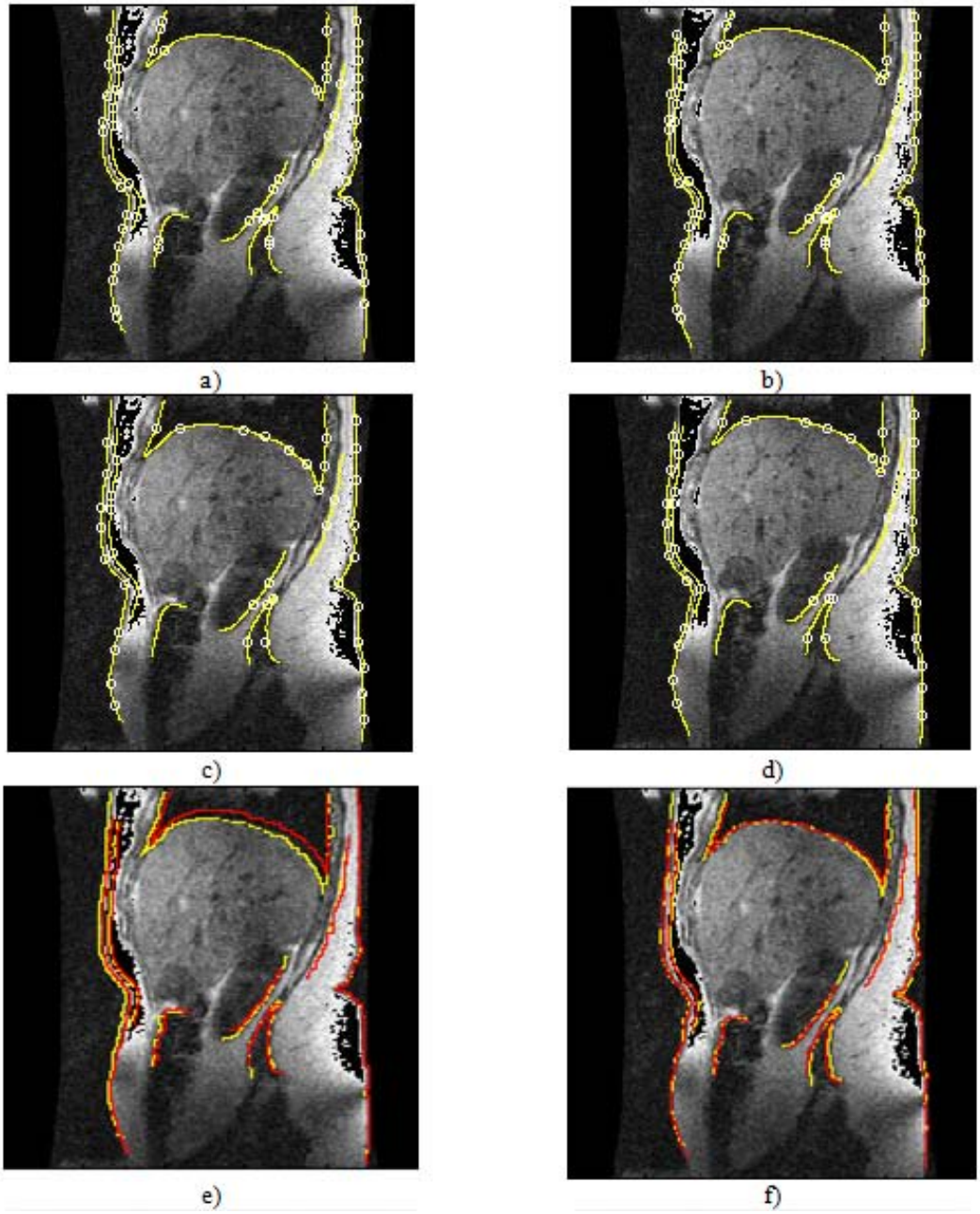

Fig.4: *a) Feature f_5 on contours of image at time $t = 0$ b) Feature f_5 on contours of image at time $t = 1$ c) Feature f_6 on contours of image at time $t = 0$ d) Feature f_6 on contours of image at time $t = 1$ e) Contours of image at time $t = 0$ (light gray) plotted with contours at time $t = 1$ (dark gray) before the alignment f) Contours of image at time $t = 0$ (light gray) plotted with contours at time $t = 1$ (dark gray) after the alignment %)*

5. B-SPLINE MODELING

5.1 B-Spline Curve

The p^{th} degree non-rational B-Spline curve is defined as follows [43][44]

$$r(t) = \sum_{i=0}^{n} N_{i,p}(t) P_i; \quad a \leq t \leq b \tag{18}$$

where the $\{P_i\}$ are the control points and $N_{i,p}(t)$ is the p^{th} -degree B-Spline basis functions defined by equation (18) defined on the non-periodic (and nonuniform) knot vector

$$U = \{\underbrace{a, ..., a}_{p+1}, u_{p+1}, ..., u_{m-p-1}, \underbrace{b, ..., b}_{p+1}\}$$

Unless stated otherwise, $a = 0$ and $b = 1$. The number of knots is related to the number of control points and the degree by the formula $m = n + p +$

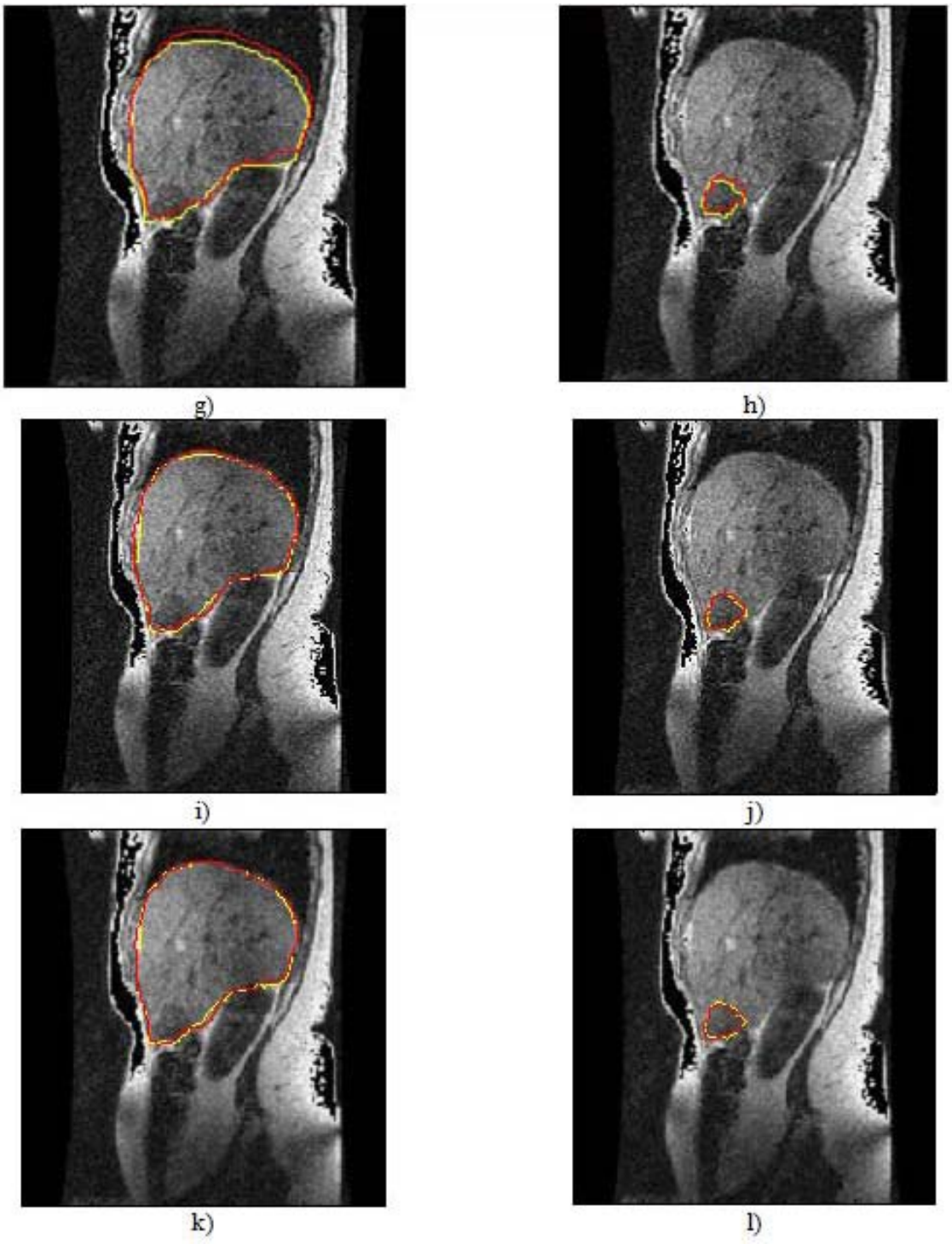

Fig.5: *g) Liver contours at time $t = 0$ (light gray) plotted with the contours at time $t = 1$ (dark gray) before the alignment (Percent Error: 5.47%) h) Liver tumor contours at time $t = 0$ (light gray) plotted with the contours at time $t = 1$ (dark gray) before the alignment (Percent Error: 15.38 i) Liver contours at time $t = 0$ (light gray) plotted with the contours at time $t = 1$ (dark gray) after the alignment using affine map (Percent Error: 2.25%) j) Liver tumor contours at time $t = 0$ (light gray) plotted with the contours at time $t = 1$ (dark gray) after the alignment using affine map (Percent Error: 7.69%) k) Liver contours at time $t = 0$ (light gray) plotted with the contours at time $t = 1$ (dark gray) after the alignment using polynomial map (Percent: 2.13%) l) Liver tumor contours at time $t = 0$ (light gray) plotted with the contours at time $t = 1$ (dark gray) after the alignment using polynomial map (Percent Error: 6.15%)*

1. The polygon formed by $\{P_i\}$ is called the control polygon. In light of the derived fiducial points in Table 1, p is at least 3, i.e., we have a cubic B-spline.

5.2 Why B-Splines

The B-Spline curve has superior properties that make them suitable for shape representation and analysis. Some of the important properties are:

(i) A B-Spline possesses a high degree of continuity important for computing the curve intrinsic properties, e.g., curvature.

(ii) Affine invariance: a B-Spline subjected to an affine transformation is still a B-Spline whose control points are obtained by subjecting the original B-Spline control points to that affine transformation.

(iii) Local shape controllability: Due to the local support of the basis B-Spline function, any local deformation is locally confined. This is very important when trying to register objects in the presence of missing parts.

(iv) Boundedness: B-Spline is bounded by the control point polygon.

6. EXPERIMENT

In this section, we apply our algorithm described previously in section 4 for intra-subject registration. We are given MRI image of liver at 24 time instances. We want to align the liver contours at different time instance, with t=0 serving as the reference. The liver contours are extracted manually by an expert. The expert also provides us the internal fiducial points of the liver. These fiducial points will be used in the verification process of the alignment, i.e., not only the external contours are aligned the internal fiducial should align as well. Figure 5.g and 5.h shows the liver contours and liver-tumor contour respectively before the alignment between time t=0 and t=1. The liver contours after the alignment using affine map are depicted in figure 5.i The liver-tumor contours after the alignment using affine map are depicted in figure 5.j The results associated with the alignment using polynomial map are shown in figure 5.k and 5.l

7. DISCUSSIONS AND CONCLUSIONS

In this paper, we introduced geometric-based methods to perform shape matching by aligning 2D sectional contours. In both cases, no iteration procedure that toggles between estimating the transformation followed by alignment was required, as we opted for geometric invariants. In 2D-to-2D alignment, we introduced a novel set of curve fiducial points which are the points on the curve where the area of parallelogram spanned by two derivative vectors vanished. To stabilize the fiducial points vis-&-vis their sensitivity to noise, we used B-Spline curve representation that smoothed out the curve prior to the computation of the fiducial points. The fiducial points were local and hence are well suited to deal with the partial alignment problem (occlusion). This is sharp contrast to other geometric invariant methods like moments and Fourier descriptors that are global in nature. In addition, the fiducial points are preserved under affine transformations (unlike other geometric features, e.g., crest lines and crest points which are only preserved under rigid transformations). To establish correspondences between the fiducial points on the two shapes, a set of absolute invariants were derived based on the areas confined between parallelograms spanned by sets of the fiducial point triplets and/or the five-point coplanar invariants. Once the correspondences were established, the parameters of a relevant transformation were estimated and the two curves were aligned. The performance of our method has been demonstrated by the ability to register for intra subject.

8. ACKNOWLEDGMENTS

This work is supported through the National Science Foundation in the US under grant number 0803670, and by King Mongkut's Institute of Technology ladkrabang (KMITL) Research Fund in Thailand.

References

[1] C. Jacobs, A. Finkelstein and D. Salesin, "Fast Multiresolution Image Query," *Computer Graphic Proceeding, SIGGARPH*, pp. 277-286, 1995.

[2] J. Z. Wang, G. Wiederhold, O. Firschein and S. X. Wei, "Wavelet-based Image Indexing Techniques with Partial Sketch Retrieval Capability," *Proceeding of the Fourth Forum on Research and Technology Advances in Digital Libraries*, IEEE, 1997.

[3] M. K. Hu, "Visual Pattern Recognition by Moment Invariants," *IRE Trans. Information Theory*, IT-8, pp. 179-187, 1962.

[4] R. J. Prokop and A. P. Reeves, "A Survey of Moment-based Techniques for Unoccluded Object Representation and Recognition," *CVGIP: Graphics Models and Image Processing*, Vol. 54, no. 5, pp. 438-460, 1992.

[5] J. Flusser and T. Suk, "Affine Moment Invariants: A New Tool for Character Recognition, " *Pattern Recognition Letters*, Vol. 15, pp. 433-436, Apr. 1994.

[6] E. L. Brill, "Character Recognition via Fourier Descriptors." WESCON Convention Record, Paper 25/3 Los Angeles, 1968.

[7] C. T. Zahn and R. Z. Zoskies, "Fourier-Descriptors for Plane Closed Curves," *IEEE Trans. Computers*, C-21, pp. 269-281, 1972

[8] P.J. Otterloo, *A contour-Oriented Approach to Shape Analysis*, Helmel Hamstead, Prentice Hall, 1992.

[9] H. Blum, "A Transformation for Extracting New Descriptors of Shape," In Whaten-Dunn, editor, Models for the Perception of Speech and Visual Forms, pp. 362-380, MIT Press, 1967.

[10] H. Blum and R. Nagel, "Shape Descriptor using Weighted Symmetric Axis Features," *Pattern Recognition*, vol. 10, pp. 167-180, 1978.

[11] S. Peleg and A. Resenfeld, "A min-max Medial Axis Transformation," *IEEE Trans. Patt. Anal. Machine Intell.*, vol. 3, pp. 208-210, 1981.

[12] P. J. Besl, " Geometric Modeling and Computer Vision," Proc. IEEE, vol. 76, pp. 936-958, Aug. 1988.

[13] V. Govindu and C. Shekhar, "Alignment using Distributions of Local Geometric Properties," *IEEE Trans. Patt. Anal. Machine Intell.*, vol. 21, no. 3, pp.1031-1043, 1999.

[14] J. Mundy and A. Zisserman. Appendix — projective geometry for machine vision. In J. Mundy and A. Zisserman, editors, *Geometric invariances in computer vision*. MIT Press, Cambridge, 1992.

[15] R. Bolles and R. Cain, "Recognizing and Locating Partially Visible Objects, The Local-Feature Focus Method," *Int'l J. Robotics. Res.*, Vol. 1, No. 3, pp. 57-82, 1982.

[16] E. E. Milios, "Shape Matching using Curvature Processes," *Comput. Vision, Graphics Image Process.*, vol. 47, pp. 203-226, 1989.

[17] C. H. Chien and J. K. Aggarwal, "Model construction and shape recognition from occluding contours," I*EEE Trans. Patt. Anal. Machine Intell.*, vol. 11, no. 4, pp. 372-389, 1989.

[18] K. K. Rao and R. Krishnan, "Shape feature extraction from object corners," *Proceedings of the IEEE Southwest Symposium on Image Analysis and Interpretation*, pp. 160-165, 1994.

[19] F. Cheikh, A. Quddus and M. Gabbouj, "Shape recognition based on wavelet-transform modulus maxima," *The 7th IEEE International Conference on Electronics, Circuits and Systems, ICECS 2000*, pp. 461-464, 2000.

[20] N. Ansari and E. J. Delp, "Partial shape recognition: a landmark-based approach," *IEEE International Conference on Systems, Man and Cybernetics*, pp. 831-836, 1989.

[21] W. S. I. Ali and F. S. Cohen, "Registering coronal histological 2-D sections of a rat brain with coronal sections of a 3-D brain atlas using geometric curve invariants and B-spline representation," *IEEE Trans. on Medical Imaging*,vol. 17, no. 6, pp. 957-966, 1998

[22] D. Shen, W. Wong and H. S. Horace, "Affine-Invaraint Image Retrieval by Correspondence Matching of Shapes," *Image and Vision Computing*, vol. 17, pp. 489-499, 1999.

[23] G. C. Stockman, S. Kopstein, and S. Benett, "Matching Images to Models for Registration and Object Detection via Clustering," *IEEE Trans. Patt. Anal. Machine Intell.*, 4, pp.229-241, 1982

[24] L. N. Kanal, B. A. Lambird, D. Lavine and G. C. Stockman, "Digital Registration of Images from Similar and Dissimilar Sensors," *Proceedings of the International Conference on Cyberbetics and Society*, pp. 347-351,1981.

[25] A. Goshtasby, "Piecewise Linear Mapping Functions for Image Registration," *Patt. recog.*, 19, 6, pp. 459-466,1986

[26] F. S. Cohen, Z. Yang, Z. Huang and J. Nissanov, "Computer Matching of Histological Rat Brain Sections," *IEEE Trans. on Biomedical Engineering* 45, 5, pp. 642-649,1998.

[27] E. Persoon and K. S. Fu, "Shape Discrimination using Fourier Descriptors," *IEEE Trans. Pattern Analysis and Mach. Intell.*, vol. PAMI-8, pp. 388-397, 1986.

[28] C. T. Zahn and R. Z. Roskies, "Fourier Descriptors for Plane Closed Curves," *IEEE Trans. Comput.*, vol. C-21, pp269-281, 1972.

[29] J. A. Saghri and H. Freeman, "Analysis of the Precision of Generalized Chain Codes for the Representation of Planar Curves," *IEEE Trans. Pattern Analysis and Mach. Intell.*, vol. PAMI-3, pp. 533-539, 1981.

[30] T. Pavlidis and F. Ali, "Computer Recognition of Handwritten Numerals by Polygonal Approximation," *IEEE Trans Sys. Man. Cybern.*, Vol SMC-6, pp 610-614, 1975.

[31] H. Asada and M. Brady, "The Curvature Primal Sketch," *IEEE Trans. Pattern Analysis and Mach. Intell.*, vol. PAMI-18, pp. 2-14, 1986.

[32] O. Philbrick, " Shape Description with the Medial Axis transformation," on Pictorial Pattern Recognition (G. C. Cheng. Ed.) Washington, DC., Thompson, 1968, pp 396-407.

[33] R. L. Kashyap and R. Chellappa, "Stochastic Models for Closed Boundary Analysis," *IEEE Trans. Inform. Theory*, vol. IT-27. pp 627-637, 1981.

[34] M. J. Paulik, M. Das and N. K. Loh, "Nonstationary Autoregressive Modeling of Object Contours, " *IEEE Trans. Signal Processing*, vol. 40, no. 3, pp. 660-675, 1992.

[35] M. K. Hu, " Vissual Pattern Recognition by Moment Invariant," *IEEE Trans. Inform. Theory*, vol.8, pp. 179-187, 1962.

[36] G. Taubin, " Estimation of Planar Curves, Surfaces, Nonplanar Surface Curve Defined by Implicit Equations with Application to Edge and Range Image Segmentation," *IEEE Trans. Pattern Analysis and Mach. Intell.*, vol. 13, no. 11, pp. 1115-1138, 1991.

[37] G. Taubin and D. Copper, "2D and 3D Object Recognition and Positioning System based on

Moment Invariant" (Reykjavik, Iceland), May 1992.

[38] J. Pones and D. J. Kriegman, "On Recognizing and Positioning Curved 3D objects from Image Contours," *Proc. IEEE Workshop Interpretation 3D Scenes*, Nov. 1989.

[39] P. J. Besl and R. C. Jain, "3D Object Reject Recognition," *Comput. Serveys*, vol. 17, no. 1, Mar. 1985.

[40] U. Grenander and D. M. Keenan, "Towards Automated Image Understanding," *Applied Statist.*, vol. 16, pp. 207-221, 1989.

[41] D. Forsyth, J. Mundy, A. Zizzerman, and C. Brown, "Projective Invariant Representation using Implicit Algrebic Curves," *Proc. Euro. Conf. Comput. Vision*. 1990.

[42] D. Keren, D. Copper and Subrahmonia, "Describing Complicated Objects by Implicit Polynomials," Reprint. LEMS Tech. Rep., Brown Univ., Oct., 1991.

[43] C. De Boor, "On Calculation with B-splines," *J. Approx. Theory*, vol. 6, pp. 50-62, 1972.

[44] C. De Boor, *A Practical Guide to Splines*, New York, Springer-Verlag, 1978.

[45] B. Kimia, *Conservation Laws and Theory of Shape*, Ph. D. Thesis, McGill Univ., 1989.

[46] M. P. Do Carmo, 1976. *Differential geometry of curves and surfaces*, Prentice hall, Englewood Cliffs, NJ.

[47] J. L. Mundy and A. Zisserman, *Geometric Invariance in Computer Vision*, MIT press, 1992.

[48] E. B. Barrett and P. Payton, "General Methods for Determining Projective Invariants in Imagery", *CVGIP: Image Understanding*, Vol. 53, No. 1, pp. 46-65, Jan. 1991.

[49] R. S. Millman and G. D. Parker, 1977. *Elements of differential geometry*. Prentice Hall, Englewood Cliffs, NJ.

[50] F. S. Cohen, W. Ibrahim and C. Pintavirooj, "Surface Modeling Using B-Splines," *IEEE Trans. on Pattern Analysis and Machine Intelligence*, Vol. 22, No. 6, pp. 642-648, June 2000.

C. Pintavirooj was born in Bangkok, Thailand in 1962. He received the B. Sc. (Radiation Techniques) and M.Sc. (Biomedical Instrumentation) from Mahidol University, Bangkok, Thailand in 1985 and 1989 respectively. In 1995, he received another master degree in Biomedical Engineering from Worcester Polytechnic Institute, MA, USA. In 2000, he earned a Ph. D.in Biomedical Engineering from Drexel University, Philadelphia, PA. After working as a research scientist at Biomedical Instrumentation Department, Mahidol University, he joined Electronic Department, Faculty of Engineering, King Mongkut's Institute of Technology at Ladkrabang, Bangkok where he is currently an associate professor. His current research is in Biomedical Image/ Signal Processing majoring in Image reconstruction, Image Classification and Image restoration. Dr. Pintavirooj is the acting chairman of Biomedical Engineering Society of Thailand affiliated with IFBME.

Fernand S. Cohen received his B.Sc. degree in physics from the American University in Cairo in 1978, and M.Sc. and Ph.D. degrees in electrical engineering from Brown University, Providence, RI, in 1980 and 1983 respectively. He joined the department of electrical engineering at the University of Rhode Island in 1983 as an assistant professor. In 1987 he joined the department of electrical and computer engineering at Drexel University, Philadelphia, PA, as a named Chair Associate Professor. He is currently a professor of Electrical and Computer Engineering and is affiliated with the School of Biomedical Engineering, Science and Health Systems, and serves as Director of Imaging and Computer Vision Center (ICVC). His research interests include medical imaging; computer vision; pattern recognition; signal processing; and applied stochastic processes.